

Effects of Seismic and Progressive Collapse Designs on the Vulnerability of RC Frame Structures

Author

Lin, Kaiqi, Li, Yi, Lu, Xinzheng, Guan, Hong

Published

2017

Journal Title

Journal of Performance of Constructed Facilities

Version

Accepted Manuscript (AM)

DOI

[10.1061/\(ASCE\)CF.1943-5509.0000942](https://doi.org/10.1061/(ASCE)CF.1943-5509.0000942)

Downloaded from

<http://hdl.handle.net/10072/370766>

Griffith Research Online

<https://research-repository.griffith.edu.au>

2 Kaiqi Lin ^a, Yi Li ^b, Xinzheng Lu ^{a,*}, Hong Guan ^c

^b Key Laboratory of Urban Security and Disaster Engineering of Ministry of Education, Beijing Collaborative Innovation Center for

5 Metropolitan Transportation, Beijing University of Technology, Beijing 100124, China.

^c Griffith School of Engineering, Griffith University Gold Coast Campus, Queensland 4222, Australia.)

Abstract: Buildings are exposed to multiple natural hazards over their service lives. Multi-hazard analysis and design of building structures has become a research hotspot worldwide. For these structures, earthquake and progressive collapse are two of the most commonly encountered hazards. However, little research has been conducted to examine the effects of the seismic and progressive collapse designs on the resistance of buildings against multiple hazards. In this study, a series of six-story reinforced concrete (RC) frames are considered and their seismic and progressive collapse designs are performed independently according to the corresponding design codes. Fragility curves are used to assess the seismic and progressive collapse resistance. The interactions between the two designs are discussed by analyzing the fragility curves and the collapse modes. Results show that the progressive collapse design of the RC frame may lead to an undesirable failure mode (i.e.,

¹ PhD Student, Key Laboratory of Civil Engineering Safety and Durability of Ministry of Education, Tsinghua Univ., Beijing 100084, China.

² Assistant Professor, Key Laboratory of Urban Security and Disaster Engineering of Ministry of Education, Beijing Univ. of Technology, Beijing 100124, China.

³ Professor, Key Laboratory of Civil Engineering Safety and Durability of Ministry of Education, Tsinghua Univ., Beijing 100084, China (corresponding author). E-mail: luxz@tsinghua.edu.cn

³ Professor, Griffith School of Engineering, Griffith Univ., Gold Coast Campus, QLD 4222, Australia.

17 “strong-beam-weak-column”) under earthquakes, which indicates that a seismic redesign is
18 necessary subsequent to the progressive collapse design. Note that sequential use of different design
19 codes for a structure may result in material waste yet a sub-optimal structural performance.
20 Therefore, a design method by individually considering different hazards is unsuitable for the
21 multi-hazard prevention and mitigation of building structures. A comprehensive and integrated
22 design method for multi-hazards is thus in great need. The outcome of this study will lay a
23 foundation for future multi-hazard analysis and design of building structures.

24 **Key words:** Multi-hazard; fragility curve; seismic design; progressive collapse design; RC frame
25 structure

26 **Introduction**

27 Building structures are exposed to multiple hazards during their service lives, such as earthquake,
28 typhoon, fire, explosion, impact etc. In some cases, different hazards may occur simultaneously or
29 immediately one after another (Ellingwood 2006, Krausmann et al. 2010). Structural safety under
30 multi-hazard environment has already drawn great attention worldwide. Nonetheless, previous
31 research studies mainly focus on the structural performance for an individual hazard (Agarwal and
32 Varma 2014, Li et al. 2014, Lu et al. 2012). Accordingly, most of the existing design methods for
33 disaster prevention and mitigation are also aimed at individual hazards. With rapid societal and
34 technological development, conventional single-hazard oriented design methods are no longer
35 viable for future advancement of civil engineering practice. It is therefore of great importance to
36 perform a multi-hazard analysis of building structures and propose a comprehensive multi-hazard
37 oriented design method (NSF 2014).

Published literature indicates that the effects of multiple hazards to buildings have been considered to some extent. Quiel & Marjanisvili (2011) evaluated the fire resistance of a damaged steel frame designed to resist progressive collapse according to the latest guidelines of the US Department of Defense (DoD). In their study, the relationship between the remaining passive fire protection and the fire-induced collapse time was discussed. Kamath et al. (2015) performed a set of full-scale loading tests on an earthquake damaged reinforced concrete (RC) frame subsequently exposed to fire, through which the residual capacity of the frame subjected to a post-earthquake fire was assessed. Formisano et al. (2015) conducted a robustness assessment for two steel framed buildings, which were respectively designed according to the old and new Italian seismic codes, under seismic loads and column removal scenarios. Jaimes et al. (2015) proposed an evaluation criterion to estimate the losses of a structure exposed to several hazards. Two middle-class houses were taken as examples to illustrate their multi-hazard assessment method. The damage rates for the two houses caused by different hazard sources including earthquakes and hurricanes were calculated. Li & Sasani (2015) and Livingston et al. (2015) evaluated the effects of seismic design and structural integrity requirement on the progressive collapse resistance of RC frames, where the effects of span length, ductility capacity and strength were also discussed. Li et al. (2011a) reviewed the state-of-the-art research progress of multi-hazard analyses from the perspective of design and evaluation, and emphasized the importance of life cycle design and the merit of multi-hazard oriented design. Most of the above-mentioned studies focused either on the response simulation or the damage/economic loss evaluation of structures under multi-hazard environment. However, to improve the structural resistance against multiple hazards, more attention must be paid to an integrated design philosophy for building structures.

60 A reliable multi-hazard oriented design is the key to improve the disaster prevention and
61 mitigation capacity of buildings. Many years of research efforts have resulted in well-developed
62 single-hazard oriented design methodologies internationally, such as the seismic design codes, fire
63 design codes and progressive collapse design codes. This allows the design of structures in resisting
64 a single hazard to be performed according to the relevant codes, whereby practical requirements can
65 be met. When multiple hazards are considered in a structural design, the current engineering
66 practice is to design the structure using different codes for individual hazards. Subsequently, the
67 individual design outcomes for different hazards are combined to yield the final design. Li et al.
68 (2011a) indicated that reducing the risk of an individual hazard may either reduce or increase the
69 structural vulnerability to other hazards. While qualitative explanations were provided in their study,
70 quantitative analyses, which are more important for engineering practices, were absent. As a matter
71 of fact, although current design codes can meet the requirement of reducing the risk of an individual
72 hazard, the correlation between different design codes is still unknown and little research work has
73 been done on this topic. Consequently, when different design codes are used one after another to
74 deal with individual hazards, it is very likely to generate an over-designed structure with redundant
75 use of construction materials; an even worse by-product could be a conflict of design outcomes
76 derived from different design codes, which may eventually weaken the overall performance of the
77 structure. Therefore, in order to reduce the multi-hazard risks of building structures, a systematic
78 assessment of the current design codes is highly desirable to quantitatively evaluate the
79 interrelationships and interactions amongst these codes, and ultimately lead to a multi-hazard
80 oriented design method.

81 In regards to the effects of a single-hazard oriented design on the structural resistance against
82 other subsequent hazards, Li & Sasani (2015) and Livingston et al. (2015) compared the progressive
83 collapse resistance of ordinary and special RC frames designed following ACI 318-11 (2011) and
84 ASCE 7 (2010). Their studies revealed that while better ductility resulted from the seismic design,
85 this design led to a weaker performance under the scenario of a column loss. Similar conclusions
86 were also made by Formisano et al. (2015), who discovered that the progressive collapse resistance
87 of a steel frame designed according to the old Italian seismic codes is better than that designed
88 using the new one. However, these existing studies only considered the effects of seismic design on
89 the structural progressive collapse resistance, whereas the interactions between the two designs for
90 both hazards have not been discussed. In addition, the evaluations of the progressive collapse
91 resistance were only performed on the component level in the three studies.

92 RC frames are one of the most widely used structural systems, having a flexible space
93 arrangement and an efficient material usage. For this reason, RC frames are selected as the focus of
94 this study. Due to large self-weight and proven fire-resistance of concrete, RC frames exhibit
95 superior wind and fire resistances (Li et al. 2015). However, the seismic resistance (Lu et al. 2012)
96 and progressive collapse resistance (Sozen et al. 1998) of RC frames are relatively weaker and
97 special designs are thus required. Two six-story RC frames, being identical in spatial arrangement
98 and plan layout but with different seismic design intensities, are studied herein. Based on the
99 evaluation of the progressive collapse resistances of the two frames, the one under a lower seismic
100 design intensity is redesigned according to the progressive collapse design code, due to its collapse
101 resistance not meeting the code requirement. Subsequently, the fragility curves are established to

102 assess the structural performances of both the original and redesigned frames under earthquake and
103 column removal scenarios. The interactions between the seismic design and progressive collapse
104 design are discussed. The analysis results show that the progressive collapse design has some
105 influence on the seismic resistance of the RC frame. This suggests that the seismic resistance is
106 necessary to be reassessed after performing the progressive collapse design. Then the seismic
107 redesign is conducted after the reassessment. Finally, the structural performance and steel
108 consumption of all these RC frames are compared. This study reveals that a sequential use of
109 different structural design codes for individual hazards would very likely result in a waste of
110 construction materials and a reduction of the global resistance against multiple hazards. The current
111 design method which considers different hazards individually is thus not applicable to multi-hazard
112 prevention and mitigation. To this end, the present study provides a scientific basis for vulnerability
113 analyses and integrated hazard design of structures in a multi-hazard environment.

114 **Study cases**

115 *Structural parameters*

116 Two structurally identical six-story RC frames are considered in this study and their elevation and
117 plan view are shown in Figure 1. For both, the first story is 4.2 m in height, and the remaining
118 stories are 3.6 m in height. Their first story columns are fully fixed to the ground. Note that such a
119 boundary condition is a commonly used idealization (Fascetti et al. 2015, Lu et al. 2013a, Ren et al.
120 2015, Tsai and Lin 2008). The dead load on each story is 5.0 kN/m², whereas the live load on each
121 story is 2.0 kN/m². The structures are designed following the Chinese design codes [i.e., the code
122 for design of concrete structures (MOHURD 2010a) and the code for seismic design of buildings

123 (MOHURD 2010b)]

124 *Seismic design of the RC frames*

125 Two study cases are derived following the two different seismic design levels, designated as RC6
126 and RC8. RC6 and RC8 have the seismic design intensities of VI and VIII, respectively. Their
127 corresponding design peak ground accelerations (PGA) with a 10% probability of exceedance in 50
128 years equal to 0.05g and 0.20g, respectively, in which g is the acceleration of gravity. The structural
129 and material parameters (gravity load, material strength, dimension of beams) of RC6 and RC8, as
130 summarized in Table 1, are kept identical as far as possible. Note that due to different requirements
131 of the maximum axial force ratios (i.e., the ratio between the design axial force and the design axial
132 resistance of the columns) specified in the Chinese seismic design code (MOHURD 2010b), the
133 column dimension in RC8 is larger than that in RC6. Specifically, the maximum axial force ratio for
134 the design intensity of VI is 0.9, while that for the design intensity of VIII is 0.75. Note that
135 different column sizes also result in different self-weights in RC6 and RC8 (Table 1). The basic
136 dynamic properties of the two frames are also given in Table 1. The reinforcement arrangement and
137 reinforcement ratio of the typical beams and columns in Zone A (Figure 1) are given in Figure 2.

138 *Numerical model and validation*

139 FE simulation has been proven to be the most widely used methodology for hazard analyses of
140 building structures (Ren et al. 2015, Xie et al. 2015, Xu et al. 2012). Published literature (Li et al.
141 2011b, Lu et al. 2012, Lu et al. 2013a, Miao et al. 2011, Ren et al. 2015) has proven that the fiber
142 beam element model, developed by Lu et al. (2013a), is capable of accurately simulating the
143 earthquake induced collapse and progressive collapse of RC frames. For this reason, FE models of
144 the two RC frames were also developed using the fiber element model in this study. It is necessary

145 to note that brittle shear failure is considered in the proposed fiber-beam model. In other words,
146 when the internal shear force exceeds the prescribed shear strength of the fiber-beam element, the
147 strength and the stiffness of the element abruptly drop to zero. However, due to the
148 “strong-shear-weak-bending” design principles in the Chinese design code (MOHURD 2010b), the
149 behavior of the structural components in this study are dominated by flexural behavior and no shear
150 failure occurs. To further validate the reliability and accuracy of the fiber beam element model in
151 the progressive collapse simulation of RC frames, a series of column removal experiments of
152 substructures of RC6 were performed (Ren et al. 2014). In these experimental tests, an edge column
153 and an interior column on the ground story (Figure 1) were removed. A 1/3-scaled ratio was adopted
154 in the tests due to the space limitation of the laboratory. Similar scale ratios were also adopted in the
155 work of Yi et al. (2008) and Qian and Li (2012a, 2012b), which have shown to have little impact on
156 the experimental results. The original dimension of the beams in RC6 is 250mm \times 500 mm in width
157 \times height and 6 m in span. The cross section of the 1/3-scaled tested beams is 85 mm \times 175 mm and
158 the span is 2 m. The test specimens were completely fixed to the strong boundary beams, which
159 have a much larger section to provide ideal fixities at boundaries. Detailed dimensions of the
160 specimens and the experimental devices are shown in Figure 3, in which the experimental areas of
161 the RC frame are also displayed. The compressive strength of concrete was 37 MPa and the yield
162 strength of reinforcement was 370 MPa. A concentrated load was applied to the beam-column joint
163 until a significant large deformation (i.e., 500 mm) was reached. More details of the experiments
164 can be found in Ren et al. (2014).

165 The tested beams are simulated using the fiber beam element, consisting of 36 concrete fibers

166 and 8 rebar fibers. The numerical simulations of the load-vertical displacement curves are compared
167 to the test results in Figure 4, with good agreement. Note that the second peaks of both curves are
168 induced by the catenary action. The comparison confirms that the fiber beam element model
169 performs fairly well in simulating the behavior of the specimens during progressive collapse,
170 especially the catenary mechanism of the specimens under large deformation. Based on such a
171 validation, this fiber beam element model is used in the subsequent simulations of this study.

172 Published literature (Tsai & Lin 2008, Yu & Tan 2013, Fragiadakis et al. 2014) indicates that
173 the complicated interaction between the slabs and the beams in resisting progressive collapse is still
174 under researched. For this reason, the slab contribution to the seismic and progressive collapse
175 resistances has often been neglected in research which has led to conservative outcomes. In this
176 study, the slab effect is also not considered to simplify the analysis. Instead, the loads on the slab
177 (including its own weight) are assigned to the supporting beams according to the load distribution
178 relationship.

179 **Design methods**

180 Two different hazard-oriented designs of the RC frames are analyzed in this study, i.e., the seismic
181 design and the progressive collapse design.

182 The seismic designs of the structures are conducted according to the Code for Seismic Design
183 of Buildings (MOHURD 2010b). The structural internal forces under seismic action are calculated
184 by the complete quadratic combination (CQC) method in which the first six vibration modes of the
185 structures are considered. The preliminary design structural internal forces are calculated by

186 combining the structural internal forces under the seismic action, wind load and gravity.
187 Consequently, the final design internal forces are obtained by adjusting the preliminary design
188 structural internal forces, to guarantee the structures exhibit the expected good mechanism to resist
189 seismic action. For example, the design bending moments of columns are amplified to achieve the
190 “strong-column-weak-beam” mechanism.

191 The progressive collapse design is conducted following the linear static alternate path (AP)
192 method regulated by GSA 2013. Specifically, the linear elastic finite element (FE) models of the RC
193 frames are established firstly. Then the columns of the RC frames are removed one after another and
194 the structural internal forces are calculated. Finally, the reinforcement in the structural members will
195 be redesigned using calculated internal forces.

196 The main differences between these two design methods are: for the progressive collapse
197 design, frame beams are significantly enhanced to resist the vertical collapse load which mainly
198 increases the reinforcement in beams; for the seismic design, beams and columns are both
199 strengthened in which the increased capacities of columns are relatively larger due to the
200 “strong-column-weak-beam” requirement.

201 **Evaluation methods**

202 To discuss the interrelationships and interactions between different design codes, it is necessary to
203 assess the structural performance under different hazards. Existing literature has documented
204 researches on both the seismic and progressive collapse performance assessments of building
205 structures (Fascetti et al. 2015, Formisano et al. 2015). The most commonly used approach to
206 describe the structural performance under different hazards with different intensities is the

207 vulnerability analysis method (Tang et al. 2011).

208 In this study, the widely accepted incremental dynamic analysis (IDA) method for earthquake
209 engineering research is used to evaluate the structural seismic performance (Lu et al 2012, Tang et
210 al. 2011). The fragility curve of a structure under different intensity ground motions can be obtained
211 through IDA, and the collapse probability (i.e., the ratio of the number of ground motions leading to
212 structural collapse to the total number of ground motions) is chosen as the vulnerability index. The
213 RC frames concerned have a regular configuration and a total height of 22.2 m, whose seismic
214 responses are dominated by the first vibration mode. Therefore, $S_a(T_1)$ (i.e., the spectral acceleration
215 at the fundamental period T_1) is chosen as the ground motion intensity measure according to Lu et
216 al. (2013b), Lu et al. (2013c) and Ye et al. (2013). Twenty-three seismic ground motions are adopted
217 for the vulnerability analysis based on Lu et al.'s work (2012). Of which, 22 ground motions are
218 selected from the far-field record set proposed in the FEMA P695 (2009) and the remaining one is
219 the widely used El-Centro 1940 record (Chopra 2001). The classical Rayleigh damping with a
220 damping ratio of 5% is also adopted.

221 Unlike seismic performance evaluation, a widely accepted vulnerability evaluation method for
222 progressive collapse is still lacking. An evaluation method similar to the IDA method is adopted in
223 this study to calculate the fragility curve of a progressive collapse. In this method, it is assumed that
224 every typical column in a structure has the same probability to fail. The progressive collapse
225 response is calculated using the nonlinear dynamic alternate path (AP) method. The collapse
226 probability (i.e. P_{collapse}) is defined as Equation (1):

$$227 \quad P_{\text{collapse}} = n_{\text{collapse}} / n_{\text{total}} \quad (1)$$

228 in which n_{collapse} is the number of cases that collapse occurs under a certain gravity load level, and
229 n_{total} is the total number of the column removal scenarios. Given random variations of the gravity
230 load on the structure, different gravity load levels are then applied to the structure (i.e., nominal
231 gravity load) during the analyses. Subsequently, the collapse probability (i.e., P_{collapse}) of the
232 structure under different nominal gravity loads can be calculated. Finally, the relationship between
233 the collapse probability and the magnitude of the nominal gravity load can be obtained. In other
234 words, a progressive collapse (due to column removal) fragility curve similar to the seismic fragility
235 curve can be derived.

236 Detailed implementation to calculate the progressive collapse fragility curve is as follows: (a)
237 According to the progressive collapse design guidelines (CECS 2014, DoD 2010, GSA 2013), every
238 column on each story of the structure is removed in turn, after the structure reaches the static
239 equilibrium under gravity load. (b) The responses of the structure after individual column removal
240 are calculated through nonlinear dynamic analysis. A vertical displacement of 1/5 span of the beam
241 is considered as the structural failure criterion (DoD 2010). (c) The gravity load on the structure is
242 changed from zero to infinity to generate the progressive collapse fragility curve subjected to
243 different nominal gravity loads.

244 **Evaluation results of RC6 and RC8**

245 Based on the vulnerability analysis method outlined above, the seismic performance and
246 progressive collapse resistance of the two RC frames, RC6 and RC8, are evaluated, using the
247 seismic and the progressive collapse fragility curves.

248 ***Evaluation of seismic performance***

249 The seismic fragility curves of RC6 and RC8 are shown in Figure 5(a), in which the x -axis is the
250 ground motion intensity $S_a(T_1)$ and the y -axis is the collapse probability. Note that the curves for
251 RD6-RD and RD6-RD2 will be discussed in the Sections “Progressive collapse design of RC6” and
252 “Redesign of RC6-RD for earthquake”. Note also that a lognormal distribution curve is used to fit
253 the collapse fragility analysis results. Here, $S_a(T_1)$ corresponds to 50 % collapse probability is
254 defined as $S_a(T_1)_{50\%}$. It is evident from the figure that $S_a(T_1)_{50\%}$ for RC6 is 0.42 g while $S_a(T_1)_{50\%}$ for
255 RC8 equals 1.38 g. This is because $S_a(T_1)_{MCE}$ (i.e., $S_a(T_1)$ for the maximum considered earthquake
256 (MCE)) for RC8 is 0.34 g (MOHURD 2010b), which is four times larger than that for RC6 (i.e.,
257 0.08 g) (MOHURD 2010b). As a result, the seismic resistance of RC8 is much greater than that of
258 RC6.

259 *Evaluation of progressive collapse resistance*

260 The progressive collapse fragility curves of the two frames are displayed in Figure 5(b) using the
261 evaluation method outlined in the Section “Evaluation methods”. Again the curves for RD6-RD and
262 RD6-RD2 will be discussed in the Sections “Progressive collapse design of RC6” and “Redesign of
263 RC6-RD for earthquake”. Note that when taking the slabs into consideration, beams will be
264 strengthened and the progressive collapse resistance will be increased according to Ren et al.
265 (2014).

266 Figure 5(b) indicates that the progressive collapse resistance of RC8 is significantly larger than
267 that of RC6. The collapse probability of RC6 and RC8 are 83.3 % and 0 %, respectively, under the
268 design gravity load (i.e., the nominal gravity equals 1.0 g). Thus, RC8 meets the requirement of
269 DoD 2010, GSA 2013 and Chinese code (CECS 2014) under the design gravity load whereas RC6

270 does not. In addition, the progressive collapse of RC6 is triggered by removing one of the columns
271 on the first to the fifth story. The collapse modes of RC6 when one of the typical columns on the
272 first story is removed are shown in Figure 6. In contrast, RC8 does not collapse at all under the
273 design gravity load, regardless of any column removal.

274 The results further suggest that a higher seismic design intensity, as for RC8, can effectively
275 improve the progressive collapse resistance. RC6, on the other hand, cannot meet the requirement
276 of progressive collapse design codes (CECS 2014, DoD 2010, GSA 2013) and an additional
277 progressive collapse design is thus necessary.

278 **Progressive collapse design of RC6**

279 *Design procedure*

280 RC6 is redesigned following the linear static alternate path (AP) method as specified in the Section
281 “Design methods”. The redesigned RC6 following the progressive collapse design procedure is
282 named as RC6-RD.

283 *Evaluation of the performance of RC6-RD*

284 As the amount of reinforcement of RC6-RD changes significantly as compared to RC6, the seismic
285 performance and progressive collapse resistance of RC6-RD will be re-evaluated.

286 *Evaluation of progressive collapse resistance*

287 The progressive collapse fragility curve of RC6-RD is presented in Figure 5(b). As evident, the
288 progressive collapse resistance of RC6-RD is significantly improved compared to RC6. Further, the
289 collapse probability is reduced to no space under the design gravity load, thereby meeting the
290 requirement of the progressive collapse design codes (CECS 2014, DoD 2010, GSA 2013).

291 *Comparison of steel consumption*

292 Note that the progressive collapse design procedure described in the Section “Progressive collapse
293 design of RC6” does not affect the reinforcement amount in the columns. The additional
294 reinforcement due to progressive collapse design is located in the beams only. A comparison of the
295 amount of longitudinal reinforcement in the beams of RC6, RC6-RD and RC8 is given in Table 2.

296 Table 2 indicates that the amount of longitudinal reinforcement in the beams of RC6 is much
297 less than that of RC8 due to the lower seismic design intensity for RC6. Subsequent to the
298 progressive collapse design, the reinforcement amount in the beams of RC6-RD increases
299 significantly compared to that in RC6. On the first to third stories of the building, the reinforcement
300 amount in the beams of RC6-RD is less than that in RC8. However, for the fourth to fifth stories,
301 RC6-RD has slightly more reinforcement in the beams than RC8. Overall, the total amount of
302 longitudinal reinforcement in RC6-RD is slightly less than that in RC8.

303 *Evaluation of seismic performance*

304 In the existing studies, design for an individual hazard only evaluates the effect of such a design on
305 the targeted hazard. However, the effects of such a design on other subsequent hazards are often
306 neglected. According to Li et al. (2011a), improving the structural resistance against an individual
307 hazard may affect the structural vulnerability to other hazards either positively or negatively.
308 Following the progressive collapse design, the reinforcement amount in RC6-RD becomes quite
309 different from that in RC6, which may affect the seismic performance of the building. Therefore, a
310 re-evaluation of the seismic performance of RC6-RD from both the component and structural levels
311 is desirable.

312 (1) Component level

313 For RC6, RC6-RD and RC8, the nominal flexural strengths at the end of the selected beams
314 (i.e. M_b) on each story are given in Table 3, in which M_b is defined following Specification 18.7.3.2
315 of ACI 318 (ACI 2014). On the first to third stories, the order of M_b is $RC8 > RC6-RD > RC6$. It
316 changes to $RC6-RD > RC8 > RC6$ on the fourth and fifth stories. This relationship is similar to the
317 distribution of the longitudinal reinforcement in frame beams along the height. This is because RC8,
318 with a higher seismic design intensity, has a 4-time larger design seismic force than RC6, the
319 reinforcement amount in RC8 is therefore mainly determined by the seismic load. In contrast, the
320 reinforcement amount in RC6 is mainly controlled by the gravity load. As a result, the M_b values of
321 RC8 are significantly larger than those of RC6. In addition, following the progressive collapse
322 design, the M_b values of RC6-RD are greatly increased and close to those of the corresponding
323 beams of RC8.

324 Note that, with an increase of nominal flexural strengths at the end of the beams (i.e. M_b), the
325 strength ratio between the nominal flexural strengths of the beams (i.e. M_b) and those of the
326 adjoining columns (i.e. M_c) changes as well. Note also that, according to the capacity design
327 principle, the columns are expected to be much stronger than the beams during earthquakes. Thus, a
328 “strong-column-weak-beam” requirement is specified in many international seismic design codes
329 (MOHURD 2010b, ACI 2014), as expressed by the following equation:

330
$$\sum M_c \geq \eta_c \sum M_b \quad (2)$$

331 in which $\sum M_c$ is the sum of the nominal flexural strengths of the columns framing into the joint,

332 $\sum M_b$ is the sum of the nominal flexural strengths of the adjoining beams, η_c is the

333 “strong-column-weak-beam” ratio. For the six-story RC frames studied herein, η_c is set as 1.2
334 according to the Chinese seismic design code (MOHURD 2010b). Note that this ratio is the same
335 for ACI 318-14 (ACI 2014).

336 The column-to-beam strength ratios at the middle joints of the RC frames (i.e., $\Sigma M_c / \Sigma M_b$) are
337 given in Table 4. Note that for the joints on the roof of the RC frames, a ratio smaller than η_c (i.e.,
338 1.2) is permitted in the Chinese seismic design code (MOHURD 2010b). The progressive collapse
339 design results in a significant increase in the flexural strengths of the beams in RC6, which may
340 violate the requirement of Equation 2. As a result, the columns in RC6-RD are relatively weaker
341 and may fail in earthquakes prior to the beams. Note that when taking slab into consideration, the
342 “strong-beam-weak-column” failure will also be more severe after the progressive collapse design
343 (Lu et al. 2012). To further illustrate this phenomenon, the seismic performance of RC6-RD is
344 re-evaluated from the structural level as presented below.

345 (2) Structural level

346 Similarly, the IDA of RC6-RD is performed and the result is presented in Figure 5(a).
347 Although the amount of longitudinal reinforcement in the beams of RC6-RD is 73.9% greater than
348 that of RC6, its seismic performance does not increase noticeably compared to that of RC6, which
349 indicates that the progressive collapse design has limited effects on the structural seismic
350 performance. The collapse PGAs of RC6 and RC6-RD under the 23 ground motions are illustrated
351 in Figure 7.

352 In general, the seismic performance of RC6-RD is close to that of RC6. Sometimes, the

353 seismic performance of RC6-RD is even worse than that of RC6. Among the 23 ground motions,
354 for 9 ground motions, the collapse PGA of RC6-RD is larger than that of RC6; for 7 ground
355 motions, the collapse PGA of RC6-RD approximately equals that of RC6; for the other 7 ground
356 motions, the collapse PGA of RC6-RD is even smaller than that of RC6. Therefore, the progressive
357 collapse design affects the structural seismic resistance. The newly added reinforcement in RC6-RD
358 may result in the “strong-beam-weak-column” failure mode and weaken the structural seismic
359 resistance, which will be further illustrated in the next section. Consequently, a seismic redesign
360 after the progressive collapse design is necessary to ensure the nominal flexural strengths of the
361 beams and columns meet the requirement of Equation 2.

362 **Redesign of RC6-RD for earthquake**

363 *Design procedure*

364 In order to prevent the “strong-beam-weak-column” failure mode from occurring after the
365 progressive collapse design, the nominal flexural strength of the columns of RC6-RD is increased
366 according to Equation 2 by adding reinforcement in the columns (MOHURD 2010b, ACI 2014).
367 The new frame with column strengthening is named as RC6-RD2.

368 *Evaluation of the performance of RC6-RD2*

369 Similarly, the structural performance of RC-RD2 is also evaluated from the perspectives of
370 progressive collapse resistance, material consumption and seismic resistance.

371 *Evaluation of the progressive collapse resistance*

372 The progressive collapse fragility curve of RC6-RD2 is given in Figure 5(b), which is shown to
373 overlap that of RC6-RD. This is because only the column reinforcement is increased in the process

374 of seismic redesign, while the reinforcement in the beams remains the same as RC6-RD. Note that
375 the progressive collapse resistance of the RC frame mainly relies on the reinforcement in the beams.
376 Consequently, the progressive collapse resistance of RC6-RD2 is essentially the same as that of
377 RC6-RD.

378 *Comparison of steel consumption*

379 A comparison of the amount of longitudinal reinforcement in the columns of RC6, RC6-RD,
380 RC6-RD2 and RC8 is shown in Table 5. After the seismic redesign, the reinforcement amount in the
381 columns of RC6-RD2 is 3.8 times larger than that of RC6 and RC6-RD, which means that more
382 reinforcement should be added to ensure that Equation 2 is satisfied.

383 *Evaluation of the seismic performance*

384 The seismic fragility curve of RC6-RD2 is shown in Figure 5(a). Following the seismic redesign,
385 the seismic performance of RC6-RD is improved significantly yet still weaker than RC8.

386 Subjected to the same FRIULI-TMZ000 ground motion, Figure 8 shows the plastic hinge
387 distribution of RC6-RD and RC6-RD2 at collapse. The seismic redesign can significantly improve
388 the failure mode of RC6 in earthquake. The plastic hinges of RC6-RD on the third to the top stories
389 are mainly located at both ends of the columns and only a limited number of plastic hinges at the
390 beam ends are observed from Axis 2 to Axis 4. Large displacements occurred on the first and
391 second stories which lead to the collapse of the entire structure. In contrast, the plastic hinge
392 distribution of RC6-RD2 is more uniform and rational. Many plastic hinges appear in the beams of
393 RC6-RD2, which dissipate more energy and significantly improve the seismic performance. The
394 collapse PGA of RC-RD2 is 1.8 g larger than that of RC6-RD under FRIULI-TMZ000 ground

395 motion. Conclusively, the seismic redesign can greatly improve the seismic resistance of RC frames
396 after performing the progressive collapse design.

397 *Comparison of the total longitudinal reinforcement consumption*

398 The total longitudinal reinforcement consumptions of the four RC frames are listed in Table 6, with
399 a descending order of $RC6-RD2 > RC8 > RC6-RD > RC6$. RC6-RD2, which is generated by the
400 progressive collapse design and the seismic redesign of RC6, has the largest steel consumption. Yet
401 its seismic performance is still weaker than RC8. This implies that more material consumption in
402 RC6-RD2 does not necessarily result in a better structural performance. Conclusively, if different
403 single-hazard oriented codes are used individually to cover multiple hazard considerations, it is very
404 likely to produce an over-designed structure with material waste yet the structural performance may
405 not be the optimum. A multi-hazard oriented design method is thus needed.

406 **Conclusion**

407 The structural safety under a multi-hazard environment has already drawn great attention worldwide.
408 A comprehensive design method catering for the complicated multi-hazard environment is
409 becoming a future trend of civil engineering research. A series of RC frames are studied in this
410 study. The progressive collapse and the seismic designs of the frames are performed and the fiber
411 beam element models of these frames are established to assess their performances. Two progressive
412 collapse experiments are simulated to validate the feasibility and reliability of the fiber beam
413 element models. Based on the validation, the vulnerability analysis method is used in this study to
414 evaluate the seismic performance and the progressive collapse resistance of the four RC frames.
415 The main conclusions are as follows:

- (1) Interactions do exist among different design codes. When the seismic design intensity of an RC frame increases from VI to VIII degree, its progressive collapse resistance will be increased as well. However, the progressive collapse design has limited effects on the structural seismic performance. Meanwhile, the progressive collapse design may result in the “strong-beam-weak-column” failure mode and weaken the structural seismic resistance. A seismic reassessment and redesign is necessary after performing the progressive collapse design.
- (2) Sequential use of different design codes in a structure may lead to material waste yet a sub-optimal performance. The RC6-RD2, which is generated by the progressive collapse design and seismic redesign of RC6, has a larger amount of longitudinal reinforcement. Yet it is still weaker than RC8 in earthquakes. The current single-hazard oriented design method is not suitable for the multi-hazard prevention and mitigation of building structures.
- (3) To achieve a resilient design of building structures in the multi-hazard environment, it is of great importance to consider all the possible hazards in the service life of building structures and propose a comprehensive and integrated multi-hazard oriented design method.

Acknowledgment

The authors are grateful for the financial support received from the National Basic Research Program of China (973 Program) (No. 2012CB719703), the National Natural Science Foundation of China (No. 51578018) and Australian Research Council through an ARC Discovery Project (DP150100606).

437 **References**

- 438 American Concrete Institute (ACI). (2011). "Building code requirements for structural concrete
439 (ACI 318-11) and commentary (318R-11)." Detroit, MI.
- 440 American Concrete Institute (ACI). (2014). "Building code requirements for structural concrete
441 (ACI 318-14) and commentary (318R-14)." Detroit, MI.
- 442 Agarwal, A. and Varma, A. H. (2014). "Fire induced progressive collapse of steel building
443 structures: The role of interior gravity columns." *Eng. Struct.*, 58, 129-140.
- 444 ASCE/Structural Engineering Institute (SEI). (2010). "Minimum design loads for buildings and
445 other structures." *SEI 7*, Reston, VA.
- 446 China Association for Engineering Construction Standardization (CECS). (2014). "Code for
447 anti-collapse design of building structures." *CECS 392: 2014*, Beijing. (in Chinese)
- 448 Chopra, A. K. (2001). *Dynamics of structures: theory and applications to earthquake engineering*.
449 Second Edition, Prentice Hall, Upper Saddle River, NJ, 245-249.
- 450 Department of Defense (DoD). (2010). "Design of structures to resist progressive collapse." *Unified*
451 *facility criteria, UFC 4-023-03*, Washington, DC.
- 452 Ellingwood, B. R. (2006). "Mitigating risk from abnormal loads and progressive collapse." *J.*
453 *Perform. Constr. Facil.*, 10.1061/(ASCE)0887-3828(2006)20:4(315), 315-323.
- 454 Fragiadakis, M., Vamvatsikos, D., and Aschheim, M. (2014). "Application of nonlinear static
455 procedures for the seismic assessment of regular RC moment frame buildings." *Earthq.*
456 *Spectra*, 30(2), 767-794.
- 457 Fascetti, A., Kunnath, S. K., and Nisticò, N. (2015). "Robustness evaluation of RC frame buildings
458 to progressive collapse." *Eng. Struct.*, 86, 242-249.
- 459 Federal Emergency Management Agency (FEMA). (2009). "Quantification of building seismic
460 performance factors." *FEMA 695*, Washington, DC.
- 461 Formisano, A., Landolfo, R., and Mazzolani, F. M. (2015). "Robustness assessment approaches for
462 steel framed structures under catastrophic events." *Comput. Struct.*, 147, 216-228.
- 463 General Services Administration (GSA). (2013). *Alternate path analysis and design guidelines for*

464 *progressive collapse resistance*. Washington, DC.

465 Jaimes, M. A., Reinoso, E., and Esteva, L. (2015). "Risk analysis for structures exposed to several
466 multi-hazard sources." *J. Earthq. Eng.*, 19(2), 297-312.

467 Kamath, P., Sharma, U. K., Kumar, V., Bhargava, P., Usmani, A., Singh, B., Singh, Y., Torero, J.,
468 Gillie, M., and Pankaj, P. (2015). "Full-scale fire test on an earthquake-damaged reinforced
469 concrete frame." *Fire Safety J.*, 73(3), 1-19.

470 Krausmann, E., Cruz, A. M., and Affeltranger, B. (2010). "The impact of the 12 May 2008
471 Wenchuan earthquake on industrial facilities." *J. Loss Prevent. Proc.*, 23(2), 242-248.

472 Li, M. and Sasani, M. (2015). "Integrity and progressive collapse resistance of RC structures with
473 ordinary and special moment frames." *Eng. Struct.*, 95, 71-79.

474 Li, Y., Ahuja, A., and Padgett, J. E. (2011a). "Review of methods to assess, design for, and mitigate
475 multiple hazards." *J. Perform. Constr. Facil.*, 10.1061/(ASCE)CF.1943-5509.0000279,
476 104-117.

477 Li, Y., Lu, X.Z., Guan, H., and Ye, L.P. (2011b). "An improved tie force method for progressive
478 collapse resistance design of reinforced concrete frame structures", *Eng. Struct.*, 33(10),
479 2931-2942.

480 Li, Y., Lu, X. Z., Guan, H., and Ye, L. P. (2014). "Progressive collapse resistance demand of RC
481 frames under catenary mechanism." *ACI Struct. J.*, 111 (5), 1225-1234.

482 Li, Y., Lu, X. Z., Guan, H., Ying, M. J., and Yan, W. M. (2015). "A case study on a fire-induced
483 collapse accident of a reinforced concrete frame-supported masonry structure." *Fire Tech.*,
484 10.1007/s10694-015-0491-0.

485 Livingston, E., Sasani, M., Bazan, M., and Sagioglu, S. (2015). "Progressive collapse resistance of
486 RC beams." *Eng. Struct.*, 95, 61-70.

487 Lu, X., Lu, X. Z., Guan, H., and Ye, L. P. (2013a). "Collapse simulation of reinforced concrete
488 high-rise building induced by extreme earthquakes." *Earthq. Eng. Struct. Dyn.*, 42(5),
489 705-723.

490 Lu, X., Lu, X. Z., Guan, H., and Ye, L. P. (2013b). "Comparison and selection of ground motion

intensity measures for seismic design of super high-rise buildings.” *Adv. Struct. Eng.*, 16(7), 1249-1262.

Lu, X., Ye, L. P., Lu, X. Z., Li, M. K., and Ma, X. W. (2013c). “An improved ground motion intensity measure for super high-rise buildings.” *Sci. China Ser. E.*, 56(6), 1525-1533.

Lu, X. Z., Ye, L. P., Ma, Y. H., and Tang, D. Y. (2012). “Lessons from the collapse of typical RC frames in Xuankou School during the great Wenchuan Earthquake.” *Adv. Struct. Eng.*, 15(1), 139-153.

Miao, Z. W., Ye, L. P., Guan, H., and Lu, X. Z. (2011). “Evaluation of modal and traditional pushover analyses in frame-shear-wall structures.” *Adv. Struct. Eng.*, 14(5), 815-836.

Ministry of Housing and Urban-Rural Development of the People’s Republic of China (MOHURD). (2010a). “Code for design of concrete structures.” *GB50010-2010*, Beijing, China.

Ministry of Housing and Urban-Rural Development of the People’s Republic of China (MOHURD). (2010b). “Code for seismic design of buildings.” *GB50011-2010*, Beijing, China.

National Science Foundation (NSF). (2014). “Decision Frameworks for multi-hazard resilient and sustainable buildings (RSB).” <http://www.nsf.gov/pubs/2014/nsf14557/nsf14557.htm?WT.mc_id=USNSF_30&WT.mc_ev=click> (Jul. 20, 2014)

Qian., K. and Li, B. (2012a). “Dynamic performance of RC beam-column substructures under the scenario of the loss of a corner column - Experimental results.” *Eng. Struct.*, 42, 154-167.

Qian., K. and Li, B. (2012b). “Slab effects on response of reinforced concrete substructures after loss of corner column.” *ACI Struct. J.*, 109(6), 845-856.

Quiel, S. E. and Marjanishvili, S. M. (2011). “Fire resistance of a damaged steel building frame designed to resist progressive collapse.” *J. Perform. Constr. Facil.*, 10.1061/(ASCE)CF.1943-5509.0000248, 402-409.

Ren, P. Q., Li, Y., Guan, H., and Lu, X. Z. (2015). “Progressive collapse resistance of two typical high-rise RC frame shear wall structures.” *J. Perform. Constr. Facil.*, 10.1061/(ASCE)CF.1943-5509.0000593, 04014087.

Ren, P. Q., Li, Y., Zhou, Y., Lu, X. Z., and Guan, H. (2014). “Experimental study on the

518 progressive collapse resistance of RC slabs.” *Proc., Structures Congress 2014*, Bell, G.R., and
519 Card, M. A. Reston, ed., American Society of Civil Engineers (ASCE), Reston, VA, 868-879.

520 Sozen, M., Thornton, C., Corley, W., and Sr., P. (1998). “The Oklahoma City Bombing: Structure
521 and Mechanisms of the Murrah Building.” *J. Perform. Constr. Facil.*,
522 10.1061/(ASCE)0887-3828(1998)12:3(120), 120–136.

523 Tang, B. X., Lu, X. Z., Ye. L. P., and Shi, W. (2011). “Evaluation of collapse resistance of RC
524 frame structures for Chinese schools in seismic design categories B and C.” *Earthq. Eng. Eng.*
525 *Vib.* 10(3), 369-377.

526 Tsai, M.H. and Lin, B.H. (2008). “Investigation of progressive collapse resistance and inelastic
527 response for an earthquake-resistant RC building subjected to column failure”. *Eng. Struct.*,
528 30(12): 3619-28. doi: 10.1016/j.engstruct.2008.05.031.

529 Xie, L. L., Lu, X. Z., Guan, H., and Lu, X. (2015). “Experimental study and numerical model
530 calibration for earthquake-induced collapse of RC frames with emphasis on key columns,
531 joints and the overall structure.” *J. Earthq. Eng.*, 10.1080/13632469.2015.1040897.

532 Xu, Z., Lu, X. Z., Guan, H., Lu, X., and Ren, A. Z. (2012). “Progressive-collapse simulation and
533 critical region identification of a stone arch bridge.” *J. Perform. Constr. Facil.*,
534 10.1061/(ASCE)CF.1943-5509.0000329, 43-52.

535 Ye, L. P., Ma, Q. L., Miao, Z. W., Guan, H., and Zhuge, Y. (2013). “Numerical and comparative
536 study of earthquake intensity indices in seismic analysis.” *Struct. Des. Tall Spec.*, 22(4),
537 362-381.

538 Yi, W. J., He, Q. F., Xiao, Y., and Kunnath, S. K. (2008). “Experimental study on progressive
539 collapse-resistant behavior of reinforced concrete frame structures.” *ACI Struct. J.*, 105(4),
540 433-439.

541 Yu, J. and Tan, K. H. (2013). “Experimental and numerical investigation on progressive collapse
542 resistance of reinforced concrete beam column sub-assemblages.” *Eng. Struct.*, 55, 90-106. doi:
543 10.1016/j.engstruct.2011.08.040

- Table 1.** Building information of RC6 and RC8
- Table 2.** Comparison of the amount of longitudinal reinforcement in beams
- Table 3.** Comparison of the nominal flexural strengths M_b at the end of the RC frame beams (unit: kN·m)
- Table 4.** The column-to-beam strength ratios at the middle joints of the RC frames (i.e., $\sum M_c / \sum M_b$)
- Table 5.** Comparison of the amount of longitudinal reinforcement in columns
- Table 6.** Total longitudinal reinforcement consumptions of the four RC frames

Table 1. Building information of RC6 and RC8

		RC6	RC8
Sections	Beam	250mm×500mm	250mm×500mm
	Column	400mm×400mm	550mm×550mm
Material consumption	Concrete (m ³) ^a	746.5	835.7
	Steel (ton) ^b	66.3	95.9
Vibration periods (s)	T_1 (1 st -order translation in X direction)	1.48	1.05
	T_2 (1 st -order translation in Y direction)	1.48	1.05
	T_3 (1 st -order torsion)	1.24	0.88
	Self-weight (ton)	2746	2955

Note: ^aConcrete: C30 ($f_c = 28.4$ MPa); ^bReinforcing steel: HRB335 ($f_y = 300$ MPa)

Table 2. Comparison of the amount of longitudinal reinforcement in beams

Story	RC6	RC6-RD		RC8	
	Reinforcement (ton)	Reinforcement (ton)	Percentage increase (%) ^a	Reinforcement (ton)	Percentage increase (%) ^a
1 st	2.20	4.04	83.9	4.67	112.8
2 nd	2.09	3.90	86.7	4.66	122.7
3 rd	1.97	3.66	86.0	4.09	108.1
4 th	1.92	3.59	87.4	3.31	73.0
5 th	1.88	3.59	94.3	2.43	29.2
6 th	1.85	1.85	0	1.98	7.1
Total	11.89	20.70	73.9	21.14	77.7

Note: ^aCompared to the reinforcement amount of RC6

Table 3. Comparison of the nominal flexural strengths M_b at the end of the RC frame beams (unit: kN·m)

Story	Location	RC6	RC8	RC6-RD
1 st	C	89	255	189.6
	M	126	308	301.6
2 nd	C	80	250	184.8
	M	121	312	294.4
3 rd	C	73	221	181.6
	M	114	282	288.8
4 th	C	66	183	180
	M	110	241	284.8
5 th	C	60	136	184.8
	M	106	191	290.4
6 th	C	62	93	62
	M	108	103	108

Note: C-Corner beam; M-Middle beam.

Table 4. The column-to-beam strength ratios at the middle joints of the RC frames (i.e., $\sum M_c / \sum M_b$)

Story	RC6	RC8	RC6-RD	RC6-RD2
1 st	1.25	1.92	0.52	1.20
2 nd	2.10	1.51	0.86	1.20
3 rd	2.37	1.53	0.93	1.20
4 th	2.28	1.57	0.88	1.20
5 th	2.05	1.41	0.75	1.20
6 th	0.93	1.06	0.93	0.93

Table 5. Comparison of the amount of longitudinal reinforcement in columns

Story	RC6 & RC6-RD		RC6-RD2		RC8	
	Reinforcement	Reinforcement	Percentage increase (%) ^a	Reinforcement	Percentage increase (%) ^a	
	(ton)	(ton)		(ton)		
1 st	1.28	4.80	274.9	5.95	365.3	
2 nd	0.79	3.89	394.6	2.01	155.3	
3 rd	0.79	3.38	329.0	2.01	155.3	
4 th	0.79	3.01	282.2	2.01	155.3	
5 th	0.79	3.87	391.2	2.01	155.3	
6 th	0.79	0.79	0	2.01	155.3	
Total	5.22	19.73	278.3	16.01	206.8	

Note: ^aCompared to the reinforcement amount of RC6

Table 6. Total longitudinal reinforcement consumptions of the four RC frames

	RC6	RC6-RD	RC6-RD2	RC8
Steel consumption (ton)	17.11	25.91	40.42	38.14

- Fig. 1.** Layout of the six-story RC frame (unit: m)
- Fig. 2.** Reinforcement details at Zone A on axis C of the RC frames (unit: mm)
- Fig. 3.** Overview of the test specimens and experimental devices (unit: mm)
- Fig. 4.** Comparisons between the numerical simulations and the test results
- Fig. 5.** Fragility curves of the RC frames
- Fig. 6.** Collapse modes of RC6 in different column removal scenarios (Nominal gravity = 1.0g)
- Fig. 7.** The seismic collapse peak ground accelerations (PGA) of RC6 and RC6-RD
- Fig. 8.** The plastic hinge distribution of RC6-RD and RC6-RD2 (Ground motion input :
FRIULI-TMZ000)

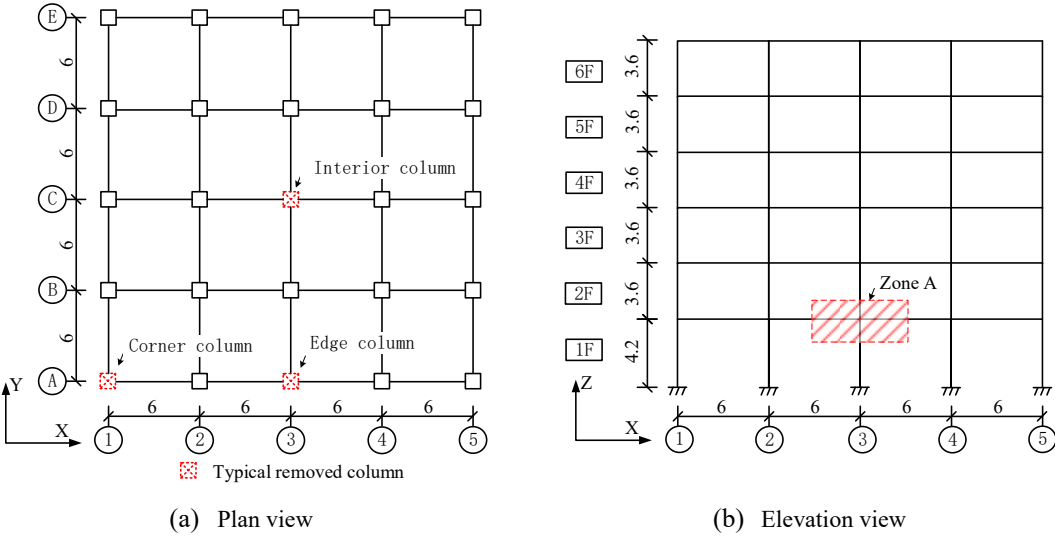
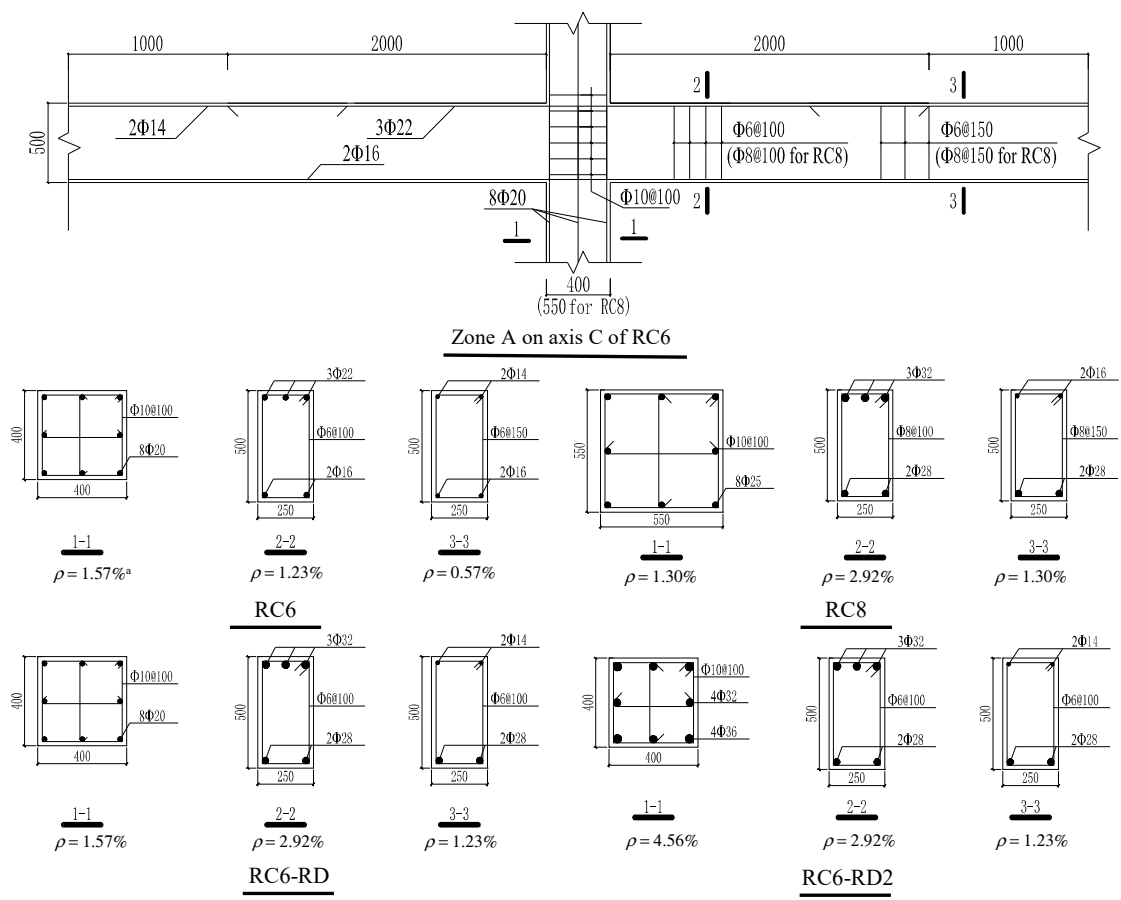


Fig. 1. Layout of the six-story RC frame (unit: m)



Note: ^a ρ : Reinforcement ratio;

Fig. 2. Reinforcement details at Zone A on axis C of the RC frames (unit: mm)

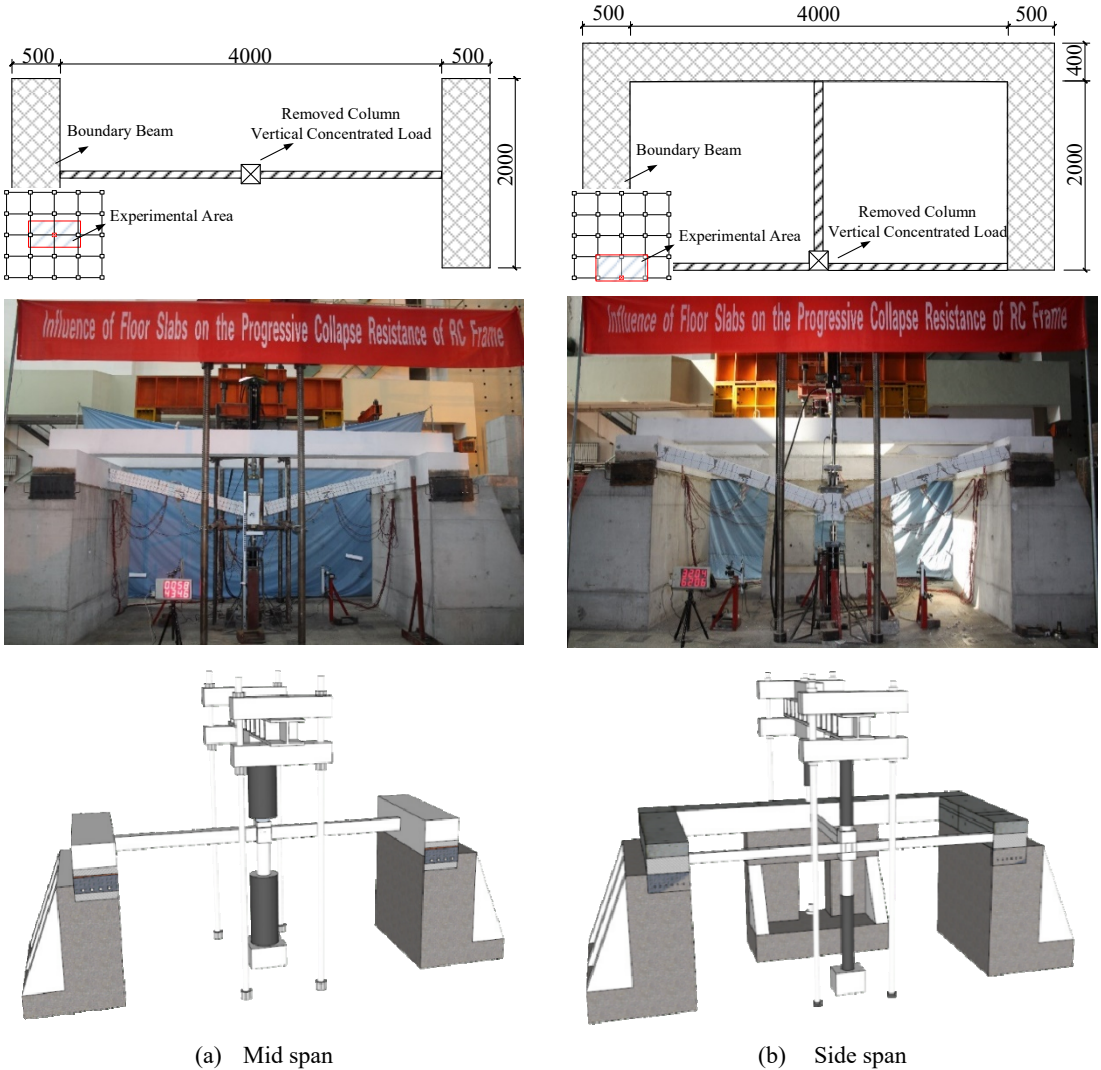


Fig. 3. Overview of the test specimens and experimental devices (unit: mm)

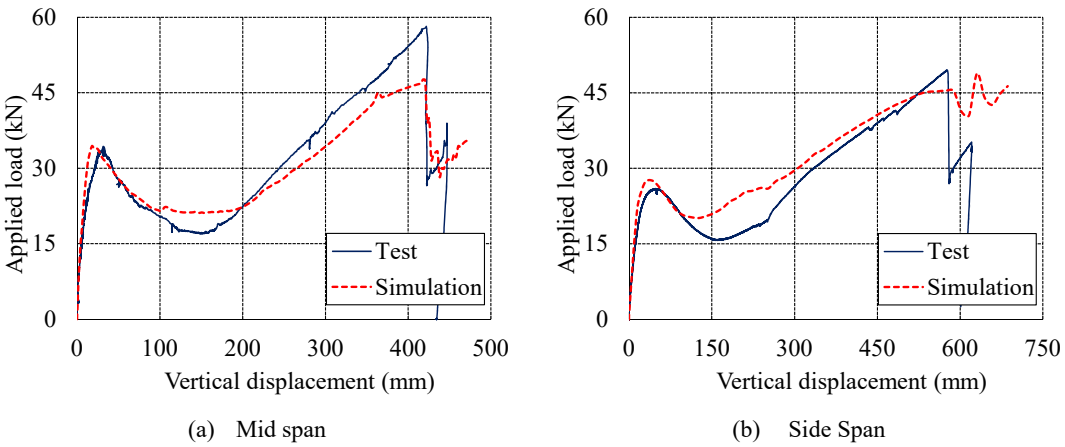
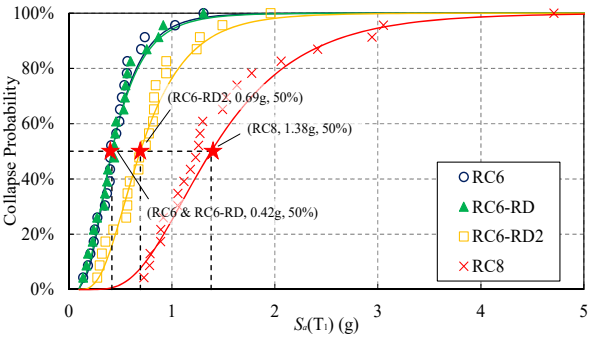
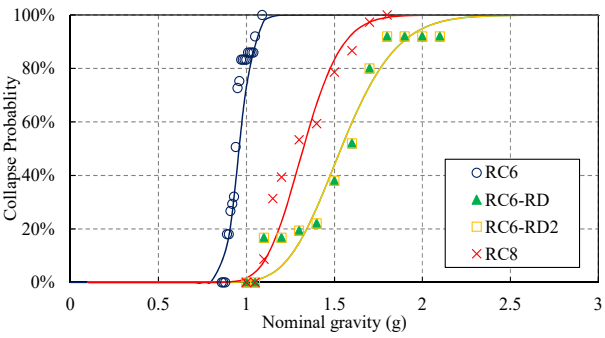


Fig. 4. Comparisons between the numerical simulations and the test results



(a) Seismic fragility curves of the RC frames



(b) Progressive collapse fragility curves of the RC frames

Fig. 5. Fragility curves of the RC frames

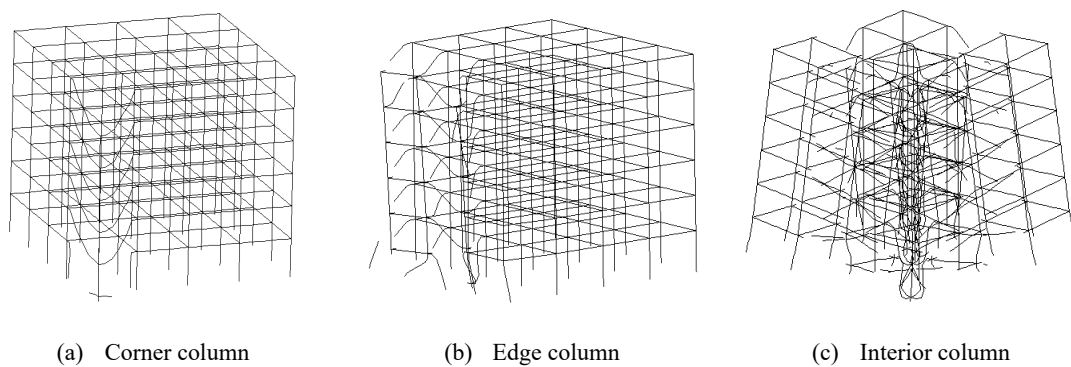


Fig. 6. Collapse modes of RC6 in different column removal scenarios (Nominal gravity = 1.0g)

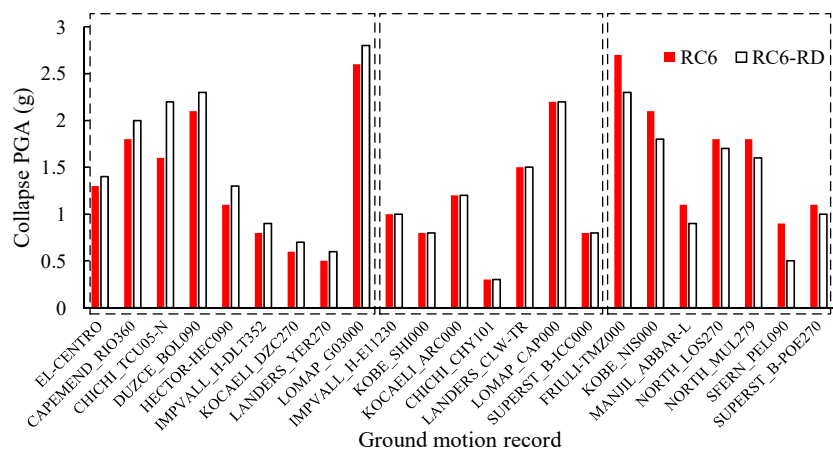


Fig. 7. The seismic collapse peak ground accelerations (PGA) of RC6 and RC6-RD

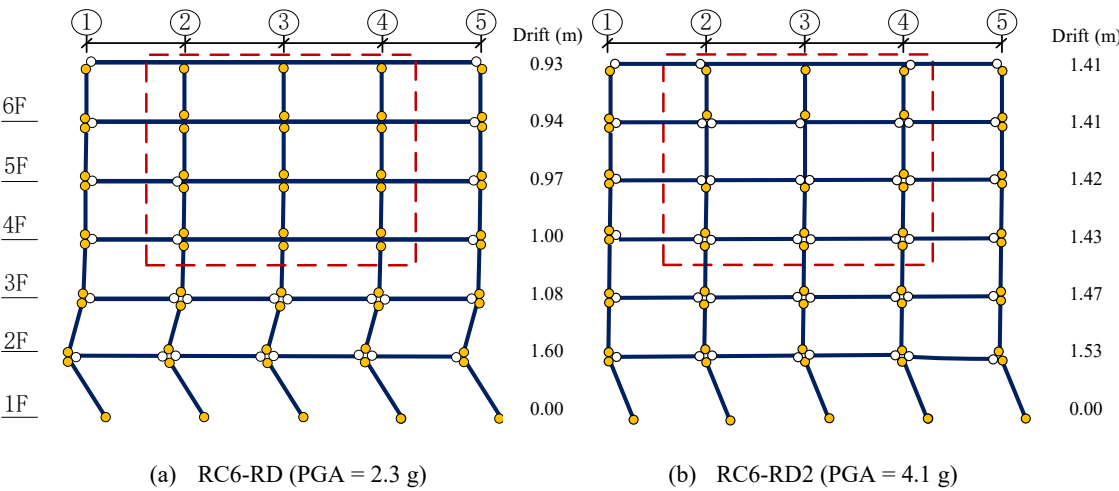


Fig. 8. The plastic hinge distribution of RC6-RD and RC6-RD2 (Ground motion input: FRIULI-TMZ000)